Clim Dyn
DOI 10.1007/s00382-009-0638-0

Impact of soil moisture initialisation and lateral boundary conditions on regional climate model simulations of the West African Monsoon

W. Moufouma-Okia · D. P. Rowell

Received: 23 February 2009 / Accepted: 15 July 2009

Abstract In this study, we use the Met Office Hadley Centre regional climate model HadRM3P to investigate the relative impact of initial soil moisture (SM) and lateral boundary conditions (LBC) on simulations of the West African Monsoon. Soil moisture data that are in balance with our particular model are generated using a 10-year (1997–2007) simulation of HadRM3P nested within the NCEP-R2 reanalyses. Three sets of experiments are then performed for six April–October seasons (2000 and 2003–2007) to assess the sensitivity to different sources of initial SM data and lateral boundary data. The results show that the only impact of the initial SM anomalies on precipitation is to generate small random intraseasonal, interannual and spatial variations. In comparison, the influence of the LBC dominates both in terms of magnitude and spatial coherency. Nevertheless, other sources of initial SM data or other models may respond differently, so it is recommended that the robustness of this conclusion is established using other model configurations.

Keywords Soil moisture initialisation · Regional climate model · Global climate model · West African Monsoon Modelling and Evaluation project · Reanalysis · Lateral boundary conditions

This paper is a contribution to the special issue on West African Climate, consisting of papers from the African Multidisciplinary Monsoon Analysis (AMMA) and West African Monsoon Modeling and Evaluation (WAMME) projects, and coordinated by Y. Xue and P. M. Ruti.

W. Moufouma-Okia (✉) · D. P. Rowell
Met Office Hadley Centre, Exeter, UK
e-mail: wilfran.moufouma-okia@metoffice.gov.uk

1 Introduction

Predicting rainfall variability is an important challenge for West Africa and especially the Sahel, a semi-arid region on the southern margin of the Sahara desert that is particularly vulnerable to both natural and anthropogenic climate fluctuations. The climate of this region is dominated by the West African Monsoon (WAM) system, which is a recurrent low latitude large-scale circulation pattern arising from the meridional boundary layer gradient of dry and moist static energy between the warm sub-Saharan continent and the tropical Atlantic Ocean (Laing and Fritsh 1993; Eltahir and Gong 1996). The Sahel has also experienced an unprecedented and severe drought from the late 1960s to the late 1980s, with partial recovery through 2003, although the rainfall deficit has not ended (Nicholson et al. 2000; L'Hote et al. 2002; Biasutti and Giannini 2006; Dai et al. 2004). Given the fragile and agriculturally based economy of West African countries, even a moderate decrease in precipitation can have serious socio-economic impacts. However, due to the chaotic nature of the climate system and its inherent timescales, atmospheric mechanisms alone cannot produce anomalies that persist for months (Lorenz 1963). Therefore, the hope for accurate climate predictions lies in the ability of the global climate models (GCMs) to simulate the atmospheric response to the slowly varying states of the ocean and land surfaces.

On interannual and decadal time scales, Sahelian rainfall has long been known to be affected by a variety of regional and global sea surface temperature (SST) anomaly patterns. These include interhemispheric contrasts of SST (Folland et al. 1986; Semazzi et al. 1988; Rowell et al. 1995), anomalies in the tropical Atlantic (Lamb 1978a, b; Hastenrath 1990; Vizy and Cook 2001; Messager et al. 2004; Paeth and Hense 2004), the east Pacific (Folland

Published online: 15 August 2009

et al. 1991; Janicot et al. 1996; Rowell 2001), the Indian ocean (Palmer 1986; Shinoda and Kawamura 1994; Rowell 2001), and the Mediterranean (Ward 1994; Rowell 2003; Jung et al. 2006). However, besides SSTs, soil moisture (SM) anomalies are believed to have a secondary influence on wet season anomalies of Sahelian rainfall, through a positive soil-precipitation feedback (Rowell et al. 1995; Douville et al. 2007). Rowell et al. (1995) and Douville (2002) show that allowing SM to evolve freely during the wet season further improves the model's response to SSTs (compared to forcing it to follow a SM climatology). According to Xue et al. (2004), the intraseasonal variability of WAM rainfall in GCM simulations could also be refined through the improvement of initial SM conditions and the SM-precipitation coupling, that is the degree to which precipitation-induced SM anomalies can feedback to the atmosphere and affect subsequent precipitation (Koster et al. 2006; Notaro 2008).

One possibility to improve climate predictions in West Africa is to use the one-way nesting Regional Climate Model (RCM) approach and account for the effects of smaller scale physiographic details such as the orography, land use distribution, and coastlines. The main idea behind this approach is to combine the large-scale response of GCMs to global forcing with the ability of RCMs to resolve smaller scale climate features (Dickinson et al. 1989; Giorgi 1990; Jones et al. 1995; Christensen et al. 1998; Giorgi and Mearns 1999; Hong and Leetma 1999; Denis et al. 2002). RCMs can also serve as experimental tools to understand regional climate processes and perform sensitivity studies (Gochis et al. 2002; Seneviratne et al. 2002; Wang et al. 2004; Vannitsem and Chomé 2005; Anya et al. 2006; Rowell and Jones 2006; Cuadra and da Rocha 2007; Yhang and Hong 2008). Although significant progress has been made in improving the physical formulation of RCMs, the most common remaining problem is the error inherited from the driving conditions, which are provided either by global analyses of observations or by GCM integrations (Noguer et al. 1998; Giorgi and Bi 2000; Seth and Rojas 2003; Rojas and Seth 2003). Note that while RCMs have been used intensively to understand the SM-precipitation linkage in mid-latitudes and over various monsoon regions (Paegle et al. 1996; Seth and Giorgi 1998; Hong and Pan 2000; Kanamitsu and Mo 2003; Anderson et al. 2006; Kim and Hong 2007; Xu et al. 2004; Nunes and Roads 2007), no attempts have been made for the WAM region. To date, RCM studies on the WAM climate have focused mainly on interannual variability, the abrupt latitudinal shift of maximum precipitation from the Guinean coast to the Sahel, and sensitivity of the July–September monsoon features to factors such as model vertical resolution, internal variability, physical parameterizations, and prescribed tropical Atlantic SSTs (Afiesimama et al. 2006; Druyan et al. 2006, 2007, 2008; Gallée et al. 2004; Jenkins 1997, Vizy and Cook 2002; Messager et al. 2004; Paeth et al. 2005; Ramel et al. 2006; Sijikumar et al. 2006; Hagos and Cook 2007; Jung and Kuntsmann 2007; Vanvyve et al. 2007).

The objective of the present study is to improve our understanding of the influence of initial SM and lateral boundary conditions (LBCs) on RCM simulations of the WAM climate in the framework of the West African Monsoon Modeling and Evaluation project (WAMME, Xue et al. 2009). This is an international initiative in conjunction with the Coordinated Enhanced Observing Period (CEOP) and the African Monsoon Multidisciplinary Analyses project (AMMA; Redelsperger et al. 2006), and investigates the role of various forcing feedbacks on the WAM dynamics using state-of-the-art GCM and RCM simulations. One objective of WAMME is to evaluate the potential for downscaling seasonal climate forecasts over West Africa. During the experimental design phase of WAMME, an important point of debate centred on the best way to specify the SM data used to initialise the seasonal RCM simulations over West Africa. This paper therefore assesses the sensitivity of the Hadley Centre RCM to the two proposed methods: one is to directly interpolate SM initial conditions from reanalysis data, and the other is to use initial SM that is in quasi-equilibrium with the RCM. We compare this SM sensitivity to the sensitivity to using differing sources of LBCs.

Section 2 provides details of the experimental design, including a brief description of the RCM and data used. An evaluation of the control simulations is given in Sect. 3. Section 4 discusses the relative impacts of initial SM and LBC on the RCM simulations. Concluding remarks follow in Sect. 5.

2 Models, data and experimental design

2.1 Regional climate model

The Met Office Hadley Centre regional climate model HadRM3P serves as the core of the PRECIS (Providing Regional Climates for Impact Study) modelling system, described in full by Jones et al. (2004). The short description given here focuses on the aspects relevant to our experiments.

HadRM3P is a high resolution limited area hydrostatic grid-point model, locatable over any part of the globe, and based on the atmospheric component of the HadCM3 coupled atmosphere–ocean GCM (Gordon et al. 2000; Pope et al. 2000) with some modifications to the model physics. There are 19 vertical levels and the latitude–longitude grid is rotated so that the equator lies inside the region of interest, in order to obtain a quasi-uniform grid box area throughout the region of interest. The horizontal resolution is 0.44° × 0.44°, which roughly corresponds to 50 km at the equator of the rotated grid, and the model timestep is 5 min.

The soil–vegetation–atmosphere interactions are of particular interest here, and are parameterized using the MOSES-1 scheme (Met Office Surface Exchange Scheme version 1; Cox et al. 1999). The associated soil model represents soil hydrology and thermodynamics using a four-layer prognostic scheme for both temperature and moisture. It includes the effects of soil water phase change and the influence of thermal and hydraulic properties. The soil layers have lower boundaries at 0.1, 0.25, 0.65 and 2.0 m which aim to resolve both the diurnal and seasonal cycles with minimal distortion. Surface runoff and soil drainage are accounted for and surface temperature is diagnosed as a skin temperature. It is assumed that only one soil and vegetation type occupies each grid box, and that the properties of the canopy store depend upon the climatological vegetation type and fractional cover within a grid box. There is also radiative heat coupling (as opposed to conductive) of the vegetated surface to the underlying soil.

2.2 Experimental design

A description of our simulations is provided here, with a summary given in Table 1. Four sets of regional climate simulations were conducted using HadRM3P to investigate model responses under different initial SM and LBC. Note that the naming convention used to denote each experiment, is such that the first part refers to the source of LBC data, and the second part refers to the source of initial SM data. Figure 1 shows the domain and orographic features of the simulations and the following three subdomains used for the analysis of experiments: Soudan–Sahel (20°W–20°E, 10°N–20°N), Guinea coast (15°W–10°E, 4°N–10°N), and East-Soudan–Sahel (20°E–30°E, 10°N–20°N). The model domain, bounded by 20°S–35°N, 35°W–35°E and containing West Africa in its centre, is the standard domain utilized in the WAMME initiative (Druyan et al. 2009), and has been used by Druyan et al. (2006, 2007) for RCM simulations of the WAM. This domain was designed to capture many important regional forcings of the WAM, including the Ahaggar-Air Mountains in northern Africa, the Tibesti and Ennedi Mountains in central Africa, and the moisture supply from the tropical Atlantic. It also attempts to avoid placing the domain boundaries over regions of complex orography (which can lead to erroneous moisture transport), and to distance the region of interest from noise generated at the outflow boundaries. The RCM domain must be large enough to allow the development of small-scale features over the area of interest, but small enough to respond to the large-scale circulations of the driving LBCs (Jones et al. 1995), unless large-scale nudging is applied (Miguez-Macho et al. 2004).

HadRM3P was first integrated continuously for 10 years (1997–2007) with the quasi-observed LBCs from the National Center for Environmental Prediction and Department of Energy Atmospheric Model Intercomparison Project Reanalysis II (NCEP-R2, Kanamitsu et al. 2002). The aim of this long-term integration, denoted NCEP_RM3PL, is to produce initial SM conditions that are fully consistent with the RCM formulation, and therefore capable of providing more appropriate estimates of initial SM moisture conditions for use in our model. In effect, we consider this experiment to be a HadRM3P-consistent reanalysis of SM, whose realism likely at least matches that of the NCEP-R2 data. The first 3 years are not used so we can be confident that SM has reached a state of quasi-equilibrium with the model atmosphere. Note that, unless specified otherwise, we refer to the NCEP_RM3PL generated SM conditions as the "balanced" SM conditions.

SM calculated by reanalyses depends on the land surface schemes used, the forcing (particularly precipitation and solar radiation), and nudging techniques. For example, ERA-40 uses a land surface scheme known as the Tiled ECMWF Scheme for Surface Exchanges over land (TESSEL, where ECMWF is the European Centre for Medium-Range Weather Forecasts; Van den Hurk et al. 2000). It has four prognostic layers for temperature and SM with the lower layer boundaries at 0.07, 0.21, 0.72, and 1.89 m. The NCEP-R2 dataset calculates SM using the two layer Oregon State University land surface model (OSU; Pan 1990) with lower boundaries at 0.1 and 1.9 m.

Three further sets of 7-month long sensitivity simulations, on which our analysis is based, were conducted using HadRM3P for the following 6 years, which have different climatic characteristics across most areas of the Sahel and portions of the Guinea coast region: the WAMME years

Table 1 Summary of the HadRM3P experiments

Experiment	Description
NCEP_RM3PL	10 year (1997–2007) continuous integration using NCEP-R2 LBCs
NCEP_RM3P	7-month integrations from 1 April for 2000, 2003–2007 using NCEPR2 LBCs and NCEP_RM3PL initial SM conditions
NCEP_ERA	As NCEP_RM3P, but uses ERA-40 initial SM
C20C_RM3P	As NCEP_RM3P, but uses LBCs from the HadAM3 climate model

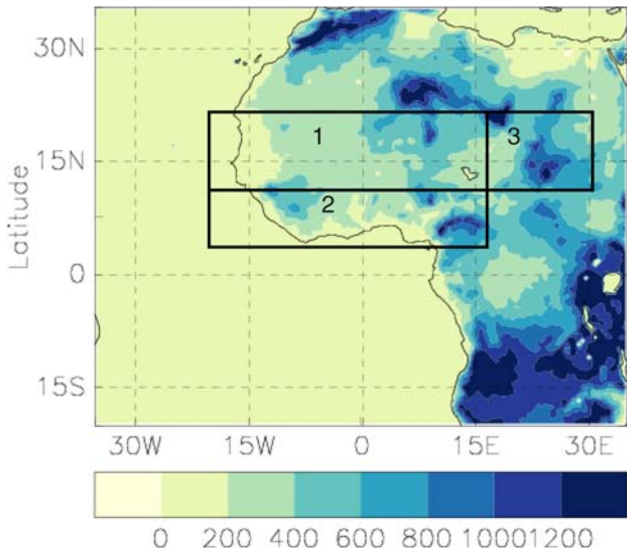

Fig. 1 Interior domain (excluding the eight-point rim) for the regional climate model experiments with terrain contour (interval of 200 m). The rectangles indicate the three subdomains used for the analysis: *1* Soudan–Sahel, *2* Guinea coast, and *3* East-Soudan–Sahel

(2000, 2003, 2004, and 2005; Xue et al. 2009), 2006 and 2007. Each individual simulation runs from April 1 to November 31, with only data from May to October (MJJASO) used for the analysis, this being the WAM monsoon season. Initial atmospheric data were selected to match each of the 6 years and to be consistent with the LBCs, so were provided by the NCEP-R2 reanalyses, except for the C20C_RM3P experiment (see below). The source of initial SM data was deliberately varied between experiments, and all initial data were linearly interpolated to the model grid. The WAMME protocol states that the month of April should be considered as a spin-up period, and so is discarded for all seasonal mean analysis. We recall that it is the aim of this paper to determine whether (for the Met Office model at least) this spin-up period is sufficient with regard to SM.

The first set of sensitivity simulations, referred to as NCEP_RM3P, is the control experiment and consists of HadRM3P seasonal integrations forced by the 6-h LBCs from the NCEP-R2 dataset and initial SM conditions from the continuous 10-year NCEP_RM3PL simulation.

The second set of simulations, referred to as NCEP_ERA, is identical to the control, except that it uses initial SM conditions from the 40-year ECMWF Reanalysis project (ERA-40, Simmons and Gibson 2000). This model configuration is similar to the standard WAMME experimental design (Druyan et al. 2009); except that here ERA-40 initial SM conditions are used instead of NCEP-R2 initial SM conditions. The main purpose of the NCEP_ERA experiment is to investigate the impact of early spring anomalous SM conditions on the subsequent monsoon precipitation over West Africa. The vertical similarity between the MOSES (HadRM3P) and TESSEL (ECMWF) land surface exchanges schemes led us to utilize initial SM conditions from ERA-40 instead of NCEP-R2 reanalyses. So we focus on the impact of differences in the horizontal distribution of initial SM—both those on large-scales due to the different climatologies of HadRM3P and ERA-40, and those on fine-scales due to the better physiographic resolution of HadRM3P—rather than on uncertainties due to the vertical interpolation of initial SM conditions.

The third set of simulations, referred to as C20C_RM3P, is identical to the control, except that it uses LBCs (and initial atmospheric data) from the Hadley Centre global atmospheric GCM (HadAM3, Pope et al. 2000; Good et al. 2008), which itself was forced by observed SSTs (see below) and integrated from 1949 to 2007. The objective of this RCM experiment is to investigate the impact of using a different LBC specification.

All experiments use identical ocean boundary conditions from the HadISST1 reconstruction of observed global SST and sea ice concentration with a 1° × 1° resolution (Rayner et al. 2003), again taking data for each of the six chosen years. These data are then processed to preserve monthly means, following Taylor et al. (2000). Maintaining the same SST forcing in all experiments isolates the relative impact of SM and LBCs on RCM simulations of the WAM, from the SST influence.

2.3 Data

The NCEP-R2 dataset supplies both the initial and lateral atmospheric boundary conditions for the reanalysis driven simulations. These data are available four times a day (00:00, 06:00, 12:00, and 18:00 UTC) with horizontal resolution of 2.5° and 17 vertical pressure levels. The variables required are relative humidity, meridional and zonal wind, surface pressure, and air temperature. In order to drive HadRM3P, the NCEP-R2 data were first interpolated from pressure levels to the RCM hybrid levels and then further processed to produce the additional prognostic variables required by HadRM3P (latent heat of cloud water and ice, water vapour, and liquid and frozen cloud water).

Given the limited availability of gridded daily rain gauge data in West Africa throughout the 6 years of the RCM integrations, the verification of model precipitation was essentially based on daily merged satellite estimates from the Global Precipitation Climatology Project (GPCP; Huffman et al. 1997) This dataset was available on a global, 1° × 1° resolution grid for the period 1996–2008. In the latitudinal band 40°N–40°S, the GPCP dataset combines the Special Sensor Microwave Imager (SSM/I) estimated fractional occurrence of precipitation with IR brightness temperatures, the latter primarily responding to clouds. McCollum et al. (2000) and Negron Juarez et al. (2009) have investigated the discrepancy between gauges and satellite estimates of precipitation in Equatorial Africa and found that GPCP estimates have twice the magnitude of rain gauge estimates. A possible explanation for this uncertainty is that convective clouds in Equatorial Africa are less maritime by nature and form under drier atmospheric conditions than most tropical cloud systems, resulting in an overestimate of the amount of satellite-derived precipitation.

The RCM simulated near-surface winds over the oceanic areas adjacent to West Africa are validated against ocean vector winds from the NASA QuikSCAT satellite. In this dataset, surface winds are derived from the microwave scatterometer SeaWinds, mounted on the QuikBird satellite. The resolution of these surface wind estimates is approximately 25 km, and they are provided as the equivalent neutral stability wind vector (that is, the wind that would produce the observed wind stress if the atmospheric boundary layer were neutrally stratified). Regardless of the atmospheric stability, surface wind stress is obtained from QuikSCAT using the bulk formula for surface drag for neutral stability as developed by Trenberth et al. (1990). From this the 10 m wind speed and direction near the sea surface can be inferred. This dataset is useful for validating our RCM in the Gulf of Guinea, compared to the quasi-model-dependent NCEP-R2 data.

3 Evaluation of control simulations

Before analysing the results of the sensitivity experiments, it is appropriate to evaluate the HadRM3P simulations of the basic features of the WAM. This section compares the mean May–October climatology of the WAM as simulated by the RCM control experiment with the available gridded observations. Due to the lack of routine observations of the troposphere, the NCEP-R2 data are used to estimate atmospheric circulation above 10 m. Of course, in data sparse regions such as West Africa, the reanalysis data is essentially a model product, but somewhat constrained by the remote observations. It is important to note that the AMMA project and intensive field experiment of the special observing period (SOP) did help to improve significantly the radiosounding network over West Africa since 2006.

3.1 Mean circulation characteristics

The rainfall regime of West Africa is modulated by the depth and northward penetration of the low level monsoon flow, which in turn depends upon the position of the mid- and upper-level jets. Therefore, assessing the simulated large-scale circulation features is an important component of validating RCM simulations of the WAM.

Figure 2 compares the mean MJJASO wind speed at 10-m for the QuikSCAT dataset and HadRM3P simulations, with the former providing an estimate of reality that is independent of the NCEP-R2 reanalysis data. The observed oceanic wind field follows a distinct spatial distribution with strong southeasterlies in the south and northeasterlies in the north. The maximum wind speed in those regions is 10 m/s. There is also a minimum of wind speed between the equator and 15°N, which corresponds to the marine location of the Intertropical Convergence Zone (ITCZ). The wind speed decreases further east in the Gulf of Guinea, with the exception of a tongue of strong wind stretching in the west–east direction off the coast of Ghana. The HadRM3P climatology agrees well with the QuikSCAT data, particularly in terms of the location and magnitude of the wind maxima that form the southwesterly monsoon flow over the Gulf of Guinea and the position of the Atlantic marine ITCZ. However, HadRM3P's flow is weaker than the satellite data in the eastern part of the Guinea Gulf, by about 2 m/s.

Figure 3 displays the mean MJJASO climatology of tropospheric circulation in the HadRM3P simulations and NCEP-R2 dataset. In the lower part of the NCEP-R2 troposphere (925 hPa), the trans-equatorial southwesterly monsoon flow prevails over the southern part of the continent, reaching 18°N and peaking over southern Nigeria with a value of 6 m/s (Fig. 3a). The northern part of the continent is dominated by the northeasterly Harmattan winds, which peak at 8 m/s near 20°N over the Darfur region. HadRM3P simulates reasonably well the extent of the moist monsoon flow and the position of the Intertropical Front (ITF, i.e. the confluence line between the moist southwesterlies and dry Harmattan winds, demarked by zero zonal wind), although wind maxima are a little stronger than those of NCEP-R2 (Fig. 3d). At 600 hPa, the NCEP-R2 mean horizontal flow is dominated by the African Easterly Jet (AEJ), which peaks over 14°N with a core speed of 12 m/s, and stretches in the zonal direction between 15°E and 15°W (Fig. 3b). The simulated HadRM3P AEJ resembles the NCEP-R2 structure but with a slightly stronger core of 14 m/s (Fig. 3e). This may suggest a slightly stronger south–north thermal gradient near the surface and transverse circulation driven by the Saharan heat low in the RCM simulations. In the upper part of the NCEP-R2 troposphere (200 hPa), the wind flow is dominated by the Tropical Easterly Jet (TEJ), which peaks over Central Africa and the Guinea coast with a value of 16 m/s, and exhibits a divergence across its main axis (Fig. 3c). The results of HadRM3P are similar, although the RCM simulated TEJ is slightly stronger (Fig. 3f). Overall the

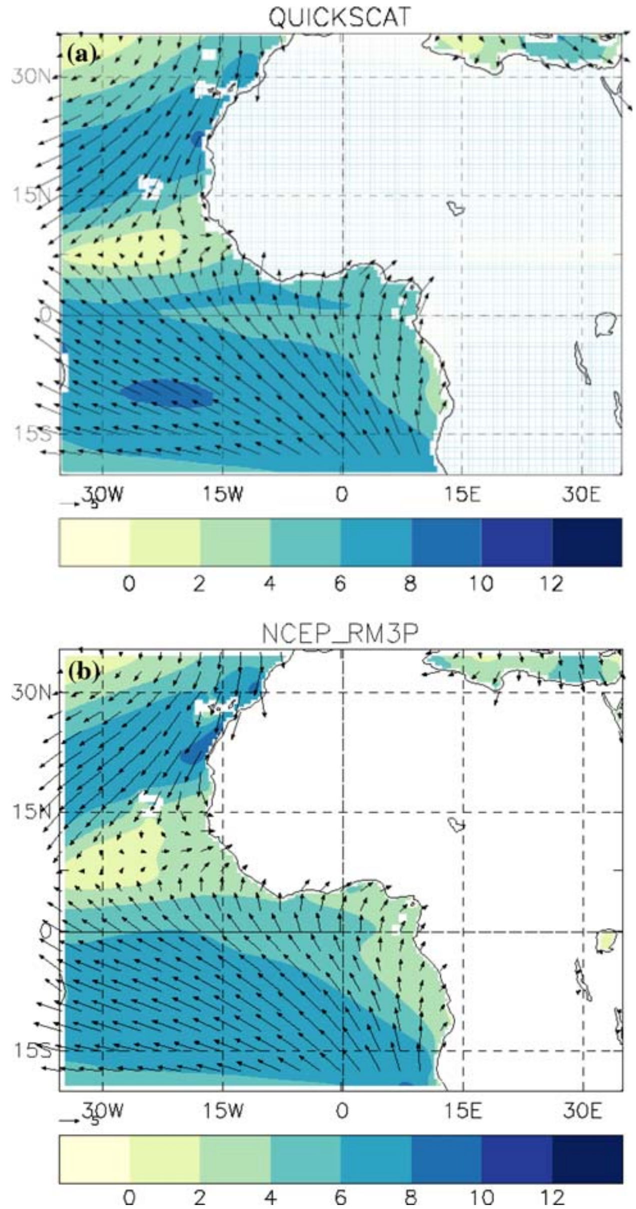

Fig. 2 Mean May–October 10-m wind (*arrows*) and magnitude of the wind (*colour shading*) in m/s for **a** QuikSCAT dataset and **b** HadRM3P averaged over the 6 years 2000, 2003–2007. *White areas* are due to missing data over land in the QuikSCAT dataset

simulated upper air circulations are also in line with results of the model intercomparison of Druyan et al. (2009), which were restricted to the four rainy seasons specified for Phase-I of WAMME.

In order to help assess the sensitivity to LBCs discussed in Sect. 4, we also present here the MJJASO climatology of the upper and lower tropospheric levels for the HadAM3 GCM (Fig. 4) and compare it with the NCEP-R2 data (Fig. 3a–c). Over the WAM area, the GCM's southwesterly monsoon flow is stronger inland than the NCEP-R2 data, but weaker further south at 5°N (Fig. 4a). The intensity of HadAM3's AEJ is similar to that of NCEP-R2, although its mean latitudinal position is a little further north (Fig. 4b), and in the upper troposphere, the TEJ core extends further west in the GCM (Fig. 4c).

3.2 Precipitation

Precipitation is one of the most important surface climate variables in monsoon areas and also the most difficult meteorological field to simulate correctly within a RCM.

Figure 5 compares the climatology of precipitation for the six MJJASO seasons in the NCEP_RM3P experiment against the observational estimates from the GPCP dataset. The model biases are presented on the $1° \times 1°$ resolution grid of the observed data, since this has a lower resolution than that of the RCM. The observed climatology shows an ITCZ punctuated by two maxima over land. One is located on the mountainous areas of Fouta-Djalon near the West African coast, and the other over the Adamaoua Massif and Cameroon highlands near the eastern part of the Gulf of Guinea (Fig. 5a). The zone of high precipitation, delineated by the 4 mm/day isohyet, stretches from the coast of Gambia to the southern part of Sudan, and is located a little south of the AEJ. The spatial correlation between the HadRM3P climatology and GPCP data is 0.92, and the root mean square error is 1.2 mm/day. Analysis of the model bias (Fig. 5c) reveals that HadRM3P underestimates the rainfall maxima around the orographic highs by 3–4 mm/day, overestimates rainfall over the Sahel, and likely produces too much rainfall over the oceanic areas adjacent to the coast. This oceanic precipitation bias, which occurs in May–June and September–October, when the ITCZ lies in the Gulf of Guinea, is also apparent in the HadAM3 driven RCM simulation (not shown), and suggests a possible deficiency in triggering moist convection along the coastal regions. This requires further investigation.

Table 2 compares the interannual anomalies of seasonal MJJASO rainfall anomalies between the GPCP estimates and the NCEP_RM3P experiment. The skill of NCEP_RM3P simulations in capturing the interannual variability of seasonal mean precipitation is relatively high in the Soudan–Sahel ($r = 0.83$) and East-Soudan–Sahel ($r = 0.92$) regions, and 'moderate' over the Guinea region ($r = 0.58$; noting that these correlations should be interpreted in a qualitative manner due to the small sample of years). This reflects the dominant influence of remote teleconnections and/or local SST anomalies on the seasonal anomalies, and suggests a mainly skillful response to these influences in the NECP-R2-HadRM3P modeling system.

Overall, the HadRM3P control simulations using balanced initial SM conditions reproduce relatively well the basic features of the WAM climatology, as well as the sign

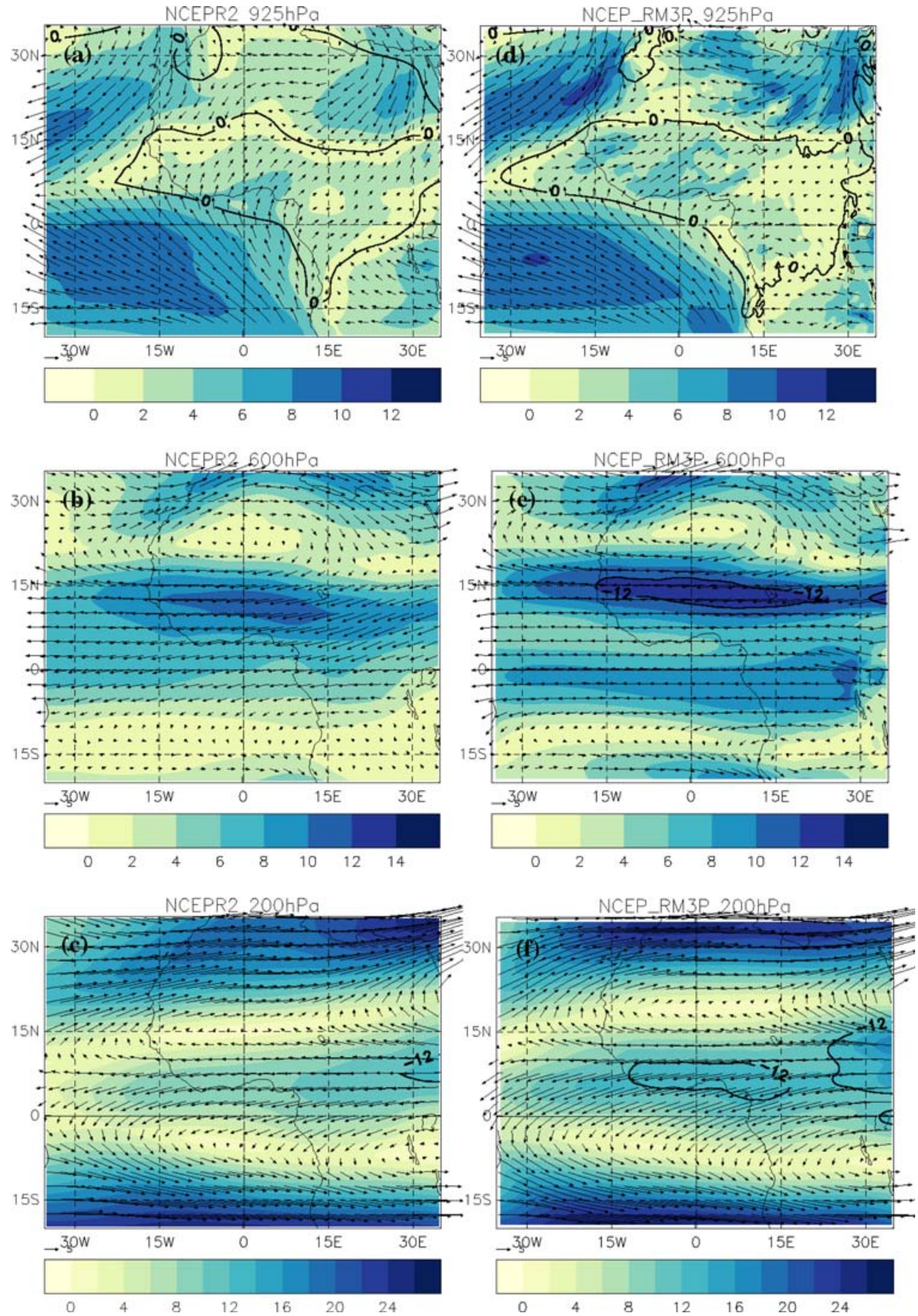

Fig. 3 Mean May–October wind (*arrows*) and magnitude of the wind (*colour shading*) in m/s at 925 hPa (*top*), 600 hPa (*middle*), and 200 hPa (*bottom*), averaged over the 6 years 2000, 2003–2007. The panels show NCEP-R2 data (*left*) and the NCEP_RM3P experiment (*right*). The *solid black line* in 925 hPa plots corresponds to the zero isoline of zonal wind which delineates the extent of the monsoon wind

(and sometimes magnitude) of the interannual anomalies of precipitation. These strong results support Druyan et al.'s (2009) comparison of WAMME participating RCMs, which showed HadRM3P achieved particularly high precipitation scores, although the simulated rainfall deficit over the Fouta Djallon and Cameroon highlands remains a common feature in many of these models. Thus, these results provide us with more confidence to use HadRM3P to perform the sensitivity experiments discussed in the following section.

4 Initial SM versus LBC sensitivity

This section documents the relative impact of using different spring initial SM conditions versus different LBCs

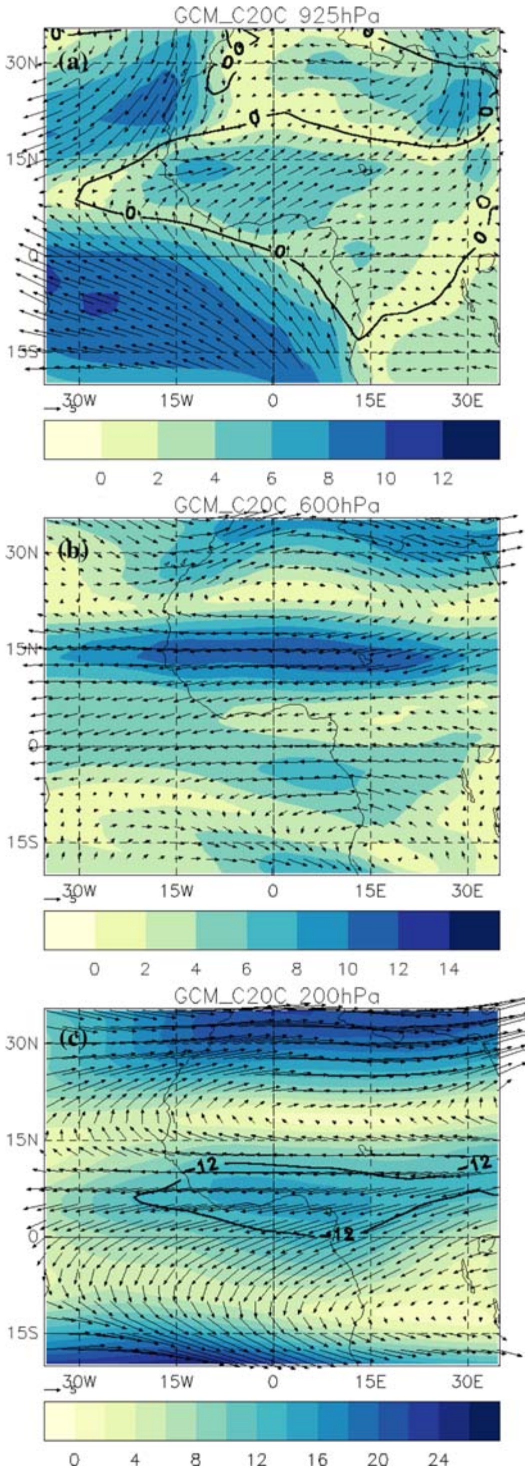

Fig. 4 Mean HadAM3 May–October wind (*arrows*) and magnitude of the wind (*colour shading*) in m/s at 925 hPa (*top*), 600 hPa (*middle*), and 200 hPa (*bottom*), averaged over the 6 years 2000, 2003–2007. The *solid black line* in 925 hPa plots corresponds to the zero isoline of zonal wind which delineates the extent of the monsoon wind

on the HadRM3P simulations of the WAM. This is achieved essentially by intercomparing the anomalies of the experiments NCEP_ERA and C20C_RM3P, with respect to the control experiment NCEP_RM3P. In Sect. 4.1 we reduce the dimensionality of the data by examining the seasonal evolution of area means, whereas in Sect. 4.2 we examine the spatial patterns of seasonal means.

4.1 Seasonal evolution

We begin by examining the evolution of the initial SM anomalies imposed on the NCEP_ERA experiments (relative to NCEP_RM3P), using time series of SM anomalies averaged over the Soudan–Sahel, East-Soudan–Sahel, and Guinea coast subdomains (Fig. 6). The results reveal large variations in the model response, depending on the depth of soil layer and subregion considered.

Over the Soudan–Sahel region, the deepest of the three analysed soil layers depicts a large positive (wet) anomaly at the start of the integration on 1 April (Fig. 6c). This positive anomaly drops rapidly from 45 kg m^{-2} (about 40% of this layer's control SM) to about half this value by the end of May, resulting from a quick removal of the SM mainly through transpiration. From June–October the wet SM anomaly decreases more gradually, and persists beyond the end of the experiment. The wet SM anomaly is also found in the second soil layer, with larger amplitude in April–August than September–October (Fig. 6b). In the top 10 cm of soil, the anomalies are relatively small in magnitude (20% of the control SM) and oscillate around zero with decreasing amplitude from April to August (Fig. 6a). The SM response over the East-Soudan–Sahel resembles that of the Soudan–Sahel (Fig. 6d–f).

The situation is different and much more striking over the Guinea coast region. First, the initial SM conditions are drier than the balanced conditions (Fig. 6g–i). Second, the SM anomaly converges to values near zero after only a month of integration, suggesting much shorter time scales of SM memory over the Guinea coast region.

Next, we examine the seasonal evolution of evapotranspiration anomalies as the means by which SM anomalies are communicated to the atmosphere and ultimately to precipitation (Fig. 7). Here, evapotranspiration corresponds to the sum of bare soil evaporation, vegetated surface evaporation, and plant transpiration. Over the Soudan–Sahel and East-Soudan–Sahel, the results indicate that the impact of initial SM on the evaporation is largest during the first few months of the experiment, April–July (Fig. 7a, b). During this period, the temporal evolution of the evaporation response is better correlated with the SM anomaly in the second (10–25 cm) soil layer ($r = 0.71$) than that of the top (0–10 cm) layer ($r = 0.43$). This is likely due to enhanced plant transpiration in response to wetter soil at the depth of plant roots over the Sahel. Over the Guinea coast, the impact of initial SM on the surface

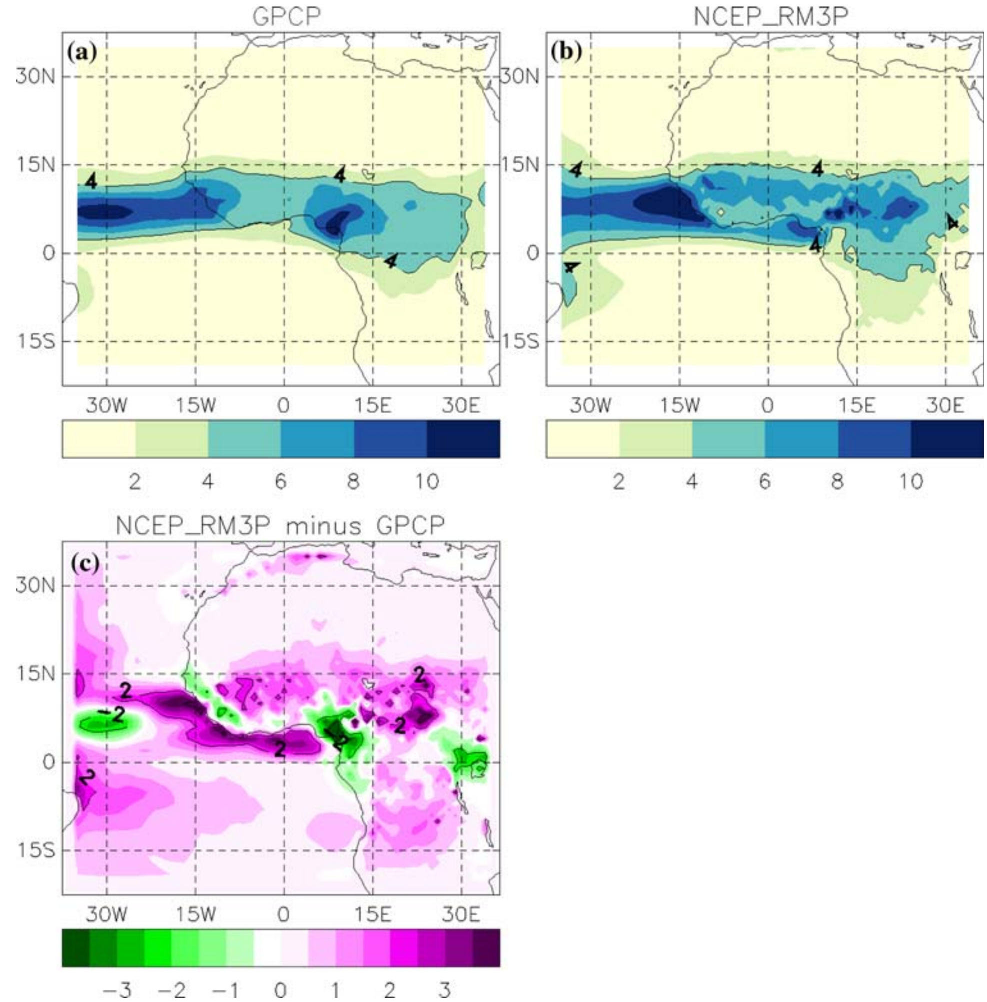

Fig. 5 Mean May–October rainfall rates in mm/day for **a** GPCP dataset, **b** the NCEP_RM3P experiment, **c** the difference NCEP_RM3P minus GPCP at 1° × 1° horizontal resolution. All data are averaged over the years 2000, 2003–2007

Table 2 MJJASO average rainfall anomaly (in mm/day) for the GPCP dataset and NCEP_RM3P experiment. The anomaly is calculated from the 6-year (2000–2007) composite climatology and averaged over the Soudan–Sahel, Guinea coast, and East-Soudan–Sahel subdomains

Years	Soudan–Sahel		Guinea		East-Soudan–Sahel	
	GPCP	HadRM3P	GPCP	HadRM3P	GPCP	HadRM3P
2000	−0.07	−0.1	−0.21	−0.12	−0.23	−0.07
2003	0.22	0.05	−0.23	0.09	0.03	0
2004	−0.25	−0.23	−0.39	−0.29	−0.28	−0.2
2005	0.12	0.12	−0.43	−0.74	−0.18	−0.04
2006	0.09	0.18	0.82	−0.01	0.31	0.2
2007	−0.19	−0.02	0.43	1.07	0.35	0.11

moisture and energy budgets is relatively weak (Fig. 7c), as illustrated by a dramatic drop in the correlations of SM with evapotranspiration in the first and second top soil layers (−0.16). This situation likely arises because evaporation over the Guinea coast is not SM limited, due to the greater availability of SM here than further north.

Figure 8 compares the 10-day running average of precipitation difference between the NCEP_ERA and NCEP_RM3P experiments, averaged over each of three selected subdomains. Over the Soudan–Sahel, notable anomalies are found throughout the experiment. However, these vary in both sign and magnitude, with no consistency between each of the 6 years, indicating that they likely arise from a chaotic response to the initial perturbations. This is further supported by a lack of temporal coherence, on a daily timescale, between these anomalies and the control rainfall rate (not shown). In other words, the initial SM perturbations lead to random atmospheric anomalies within the RCM domain, which have a greater impact on rainfall than any systematic influence of the initial SM anomalies. The precipitation response over the East-Soudan–Sahel is very similar to that of the Soudan–Sahel; except that the amplitude of the chaotic anomalies is reduced in August–October (Fig. 8b). The picture is again similar over the Guinea coast region, although here the lack of any systematic response to the initial SM is expected from the lack of evaporative response discussed earlier.

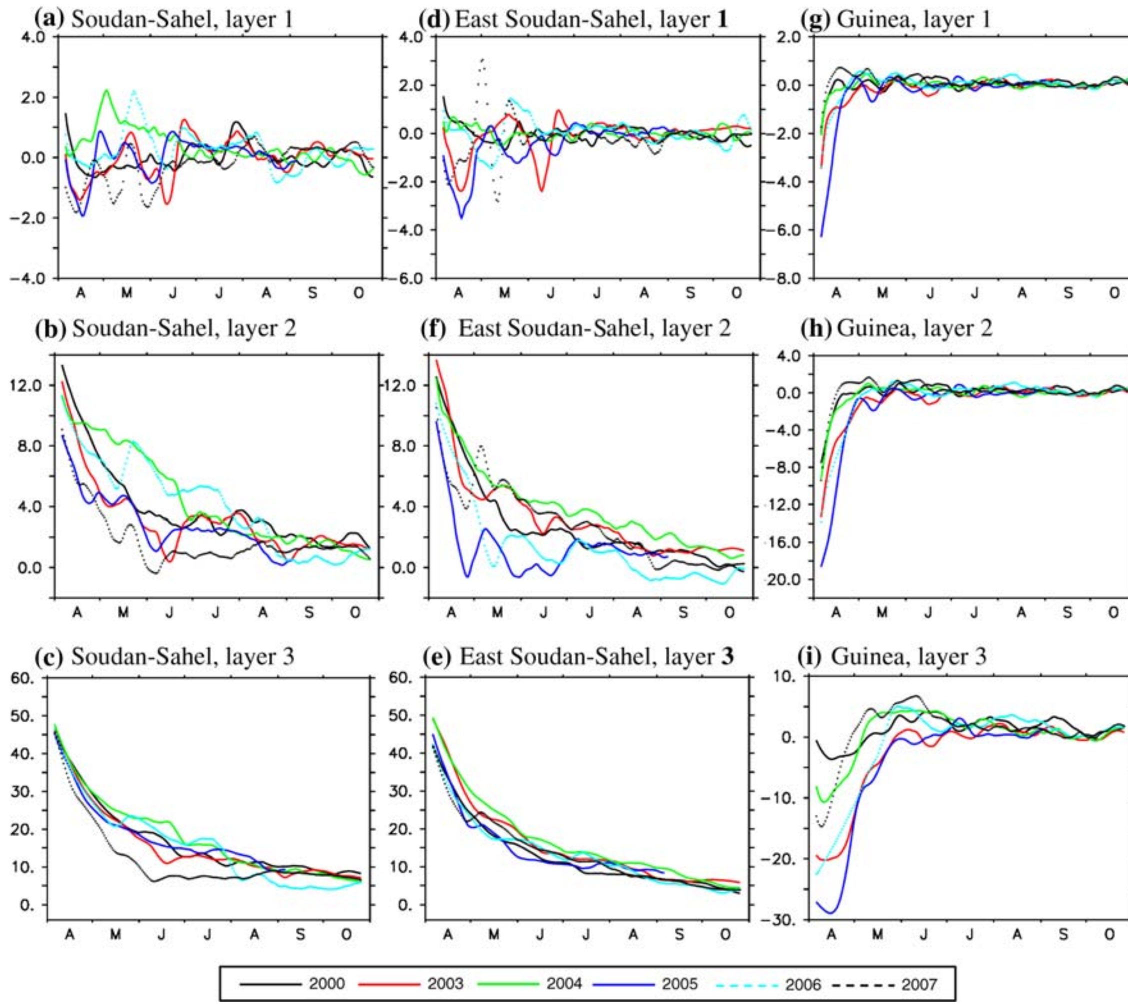

Fig. 6 Ten-day running average of soil moisture anomalies in NCEP_ERA experiment (computed as NCEP_ERA minus NCEP_RM3P, in kg m^{-2}) for the Soudan–Sahel (*left*), East-Soudan–Sahel (*centre*), and Guinea coast (*right*). From top to bottom, the panels show the first, second and third model soil layers. The lines show the seasonal evolution (April–October) for individual years (see key)

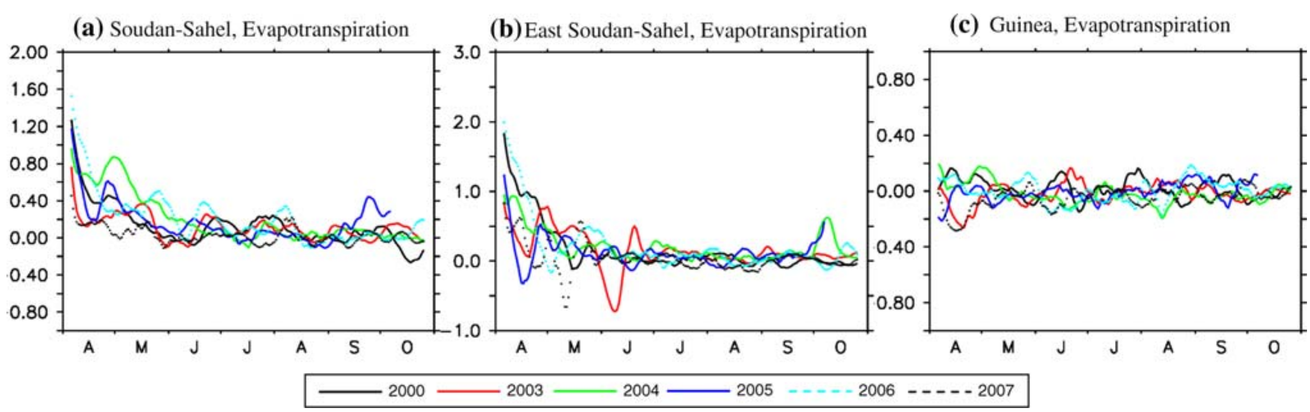

Fig. 7 Ten-day running average of evapotranspiration anomalies (mm/day) in NCEP_ERA simulations (computed as NCEP_ERA minus NCEP_RM3P). The panels show the Soudan–Sahel (*left*), East-Soudan–Sahel (*centre*), and Guinea coast (*right*) regions. The *lines* show the seasonal evolution (April–October) for individual years (see key)

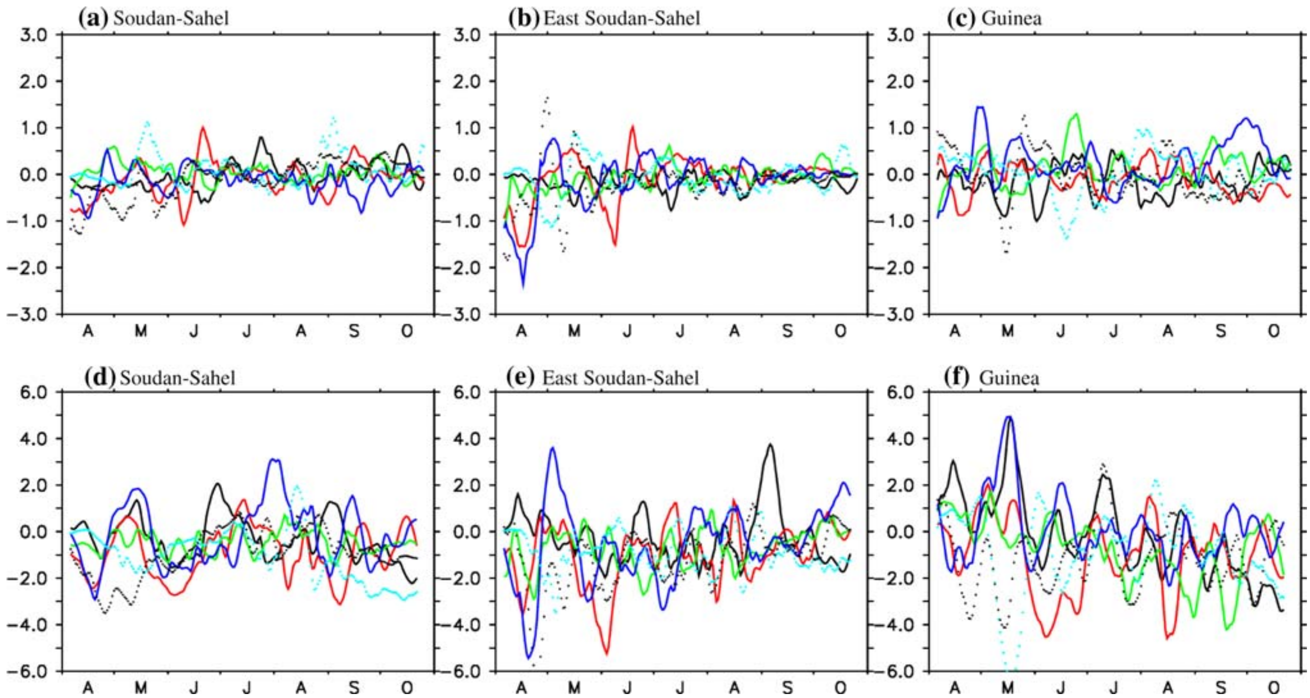

Fig. 8 Ten-day running average of the precipitation anomalies (mm/day) in NCEP_ERA (*top*) and C20C_RM3P (*lower*) experiments, with respect to NCEP_RM3P experiments. Panels display results over the Soudan–Sahel (*left*), East-Soudan–Sahel (*centre*), and Guinea coast (*right*). The *lines* show the seasonal evolution (April–October) for individual years (see key)

Figure 8d–f display the 10-day running average of the precipitation response due to changes of LBCs. Overall the impact of LBCs is larger than that of SM initialisation (note the vertical scales on the panels) and persists throughout the entire simulation period, although it varies from year to year. Both the intraseasonal variability and the seasonal totals are affected. The impact on the former is apparent in Fig. 8, where the magnitude of the 10-day precipitation response ranges from −5 to 4 mm/day, due in part to the different timing of synoptic disturbances and other perturbations arriving in the RCM region from the LBCs. Figure 9 demonstrates that the probability distribution (PDF) of the intensity of these rainfall events is also affected by the change in LBCs, with weak rainfall events occurring more frequently in all regions using HadAM3 LBCs and moderate events occurring less frequently. These PDFs are much less affected when only the SM initialization is altered (Fig. 9). Similarly, systematic differences in seasonal mean rainfall (Table 3) also result from the different climatologies of the two driving models (Figs. 3, 4), although a detailed understanding of this response will require further investigation.

4.2 Spatial pattern

Further understanding of the relative impacts of LBCs and initial SM conditions on mean seasonal precipitation can be gained if we investigate the horizontal distribution of the anomalies.

The pattern of seasonally averaged (May–October) precipitation anomalies induced from using the unbalanced initial SM conditions is shown in Fig. 10, and reveals substantial spatial and interannual variations in both the sign and magnitude of the response on a range of spatial scales. This contrasts with the pattern of the initial SM anomaly (not shown) which has much greater spatial coherence, with positive anomalies over the (East-) Soudan–Sahel and negative anomalies farther south. This therefore reinforces the conclusion of the previous section, that the initial SM perturbations induce only chaotic anomalies within the RCM domain, rather than any systematic influence. Note that these random responses to initial SM also influence rainfall over the ocean, with some anomalies having quite large spatial coherence, suggesting a further chaotic impact on circulation anomalies linked to the WAM.

Also shown are the patterns of seasonally averaged precipitation anomalies resulting from the change of LBCs in the six studied years (Fig. 11). Overall, the use of large scale driving conditions from HadAM3 reduces dramatically the precipitation over most of West and Central Africa. The precipitation deficit rises up to 4 mm/day in some years and some locations. Compared to initial SM conditions, the LBCs have a greater impact, greater spatial

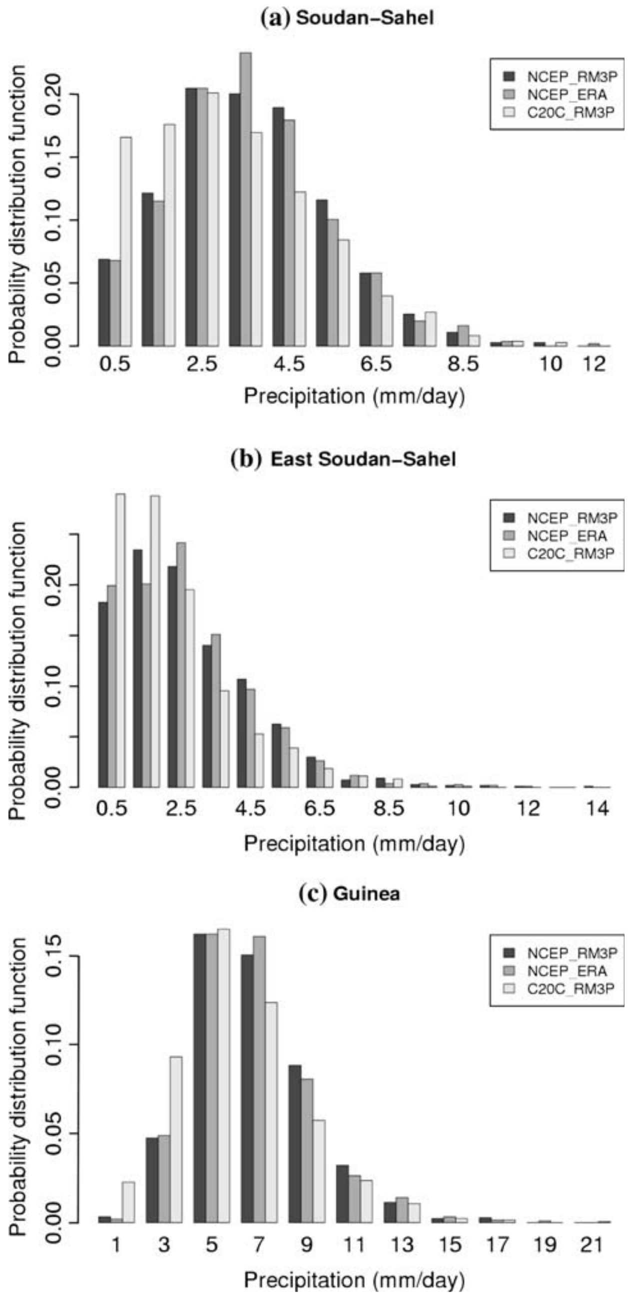

Fig. 9 Probability distribution of daily precipitation rates (mm/day) in NCEP_RM3P, NCEP_ERA, C20C_RM3P experiments. Data cover the entire season May–October for the years 2000, 2003–2007. The panels show the Soudan–Sahel (*top*), East-Soudan–Sahel (*middle*), and Guinea (*bottom*) regions

coherency, and less interannual variability. Note that the mean seasonal precipitation pattern of the C20C_RM3P simulations was assessed for realism against the GPCP data (not shown). The results indicate some similarities with the errors found in the control simulations over land (Fig. 5c), except that there is much less precipitation in the belt of maximum rainfall (consistent with Fig. 11).

Table 3 Comparison of MJJASO average rainfall (for 2000, 2003–2007, in mm/day) and rainfall anomalies (differences from NCEP_RM3P, as a percentage of NCEP_RM3P data) for each RCM experiment

Region	NCEP_RM3P	NCEP_ERA		C20C_RM3P	
	Mean	Mean	Anomaly	Mean	Anomaly
Soudan–Sahel	3.63	3.61	−1	3.05	−16
East Soudan–Sahel	2.71	2.67	−1	2.10	−23
Guinea	6.75	6.76	0	5.92	−12

5 Conclusions

Despite significant progress in using RCM, little is known on the relevance of initial SM uncertainties for predicting the WAM climate. Much more attention has been given to the uncertainties associated with model physical formulations and LBCs. In this study, we use the Met Office Hadley Centre regional climate model HadRM3P to investigate the relative impact of initial SM and LBCs on the simulated WAM seasonal and intraseasonal variability, with an emphasis on precipitation. First, a 10-year (1997–2007) continuous integration was conducted with the NCEP-R2 LBCs in order to generate a reanalysis of SM that is in balance with HadRM3P. Three additional sets of 7-month simulations were conducted for April–October 2000, 2003, 2004, 2005, 2006 and 2007. The control simulations were nested within NCEP-R2 LBCs and used the balanced initial SM. The second set of simulations used initial SM from the ERA reanalyses, and the third set of simulations used LBCs from a GCM (HadAM3).

The control experiment is broadly consistent with both observations and the driving LBCs. It simulates relatively well the monsoon area, and the positions of the ITF, AEJ at 600 hPa, and TEJ at 200 hPa, but does appear to slightly overestimate the magnitude of the wind maxima. The spatial correlation between the RCM and GPCP precipitation is high (0.92), but the model underestimates the rainfall maxima around the orographic highs by 3–4 mm/day. The NCEP-R2 driven RCM skill for capturing the interannual variability of seasonal mean precipitation is high over the Soudan–Sahel and East-Soudan–Sahel, but more moderate over the Guinea coast. Overall, this performance at least matches that of other RCMs used in the WAMME model intercomparison of Druyan et al. (2009).

The analysis of the response to early spring initial SM anomalies reveals many distinct features. Over the Soudan–Sahel and East-Soudan–Sahel, the initial SM anomalies persist for several months after the start of the simulation, although with gradually decaying magnitude. This then affects evapotranspiration, but in the experiments

Fig. 10 MJJASO mean precipitation difference, NCEP_ERA minus NCEP_RM3P, (mm/day) for each of the years 2000, 2003–2007

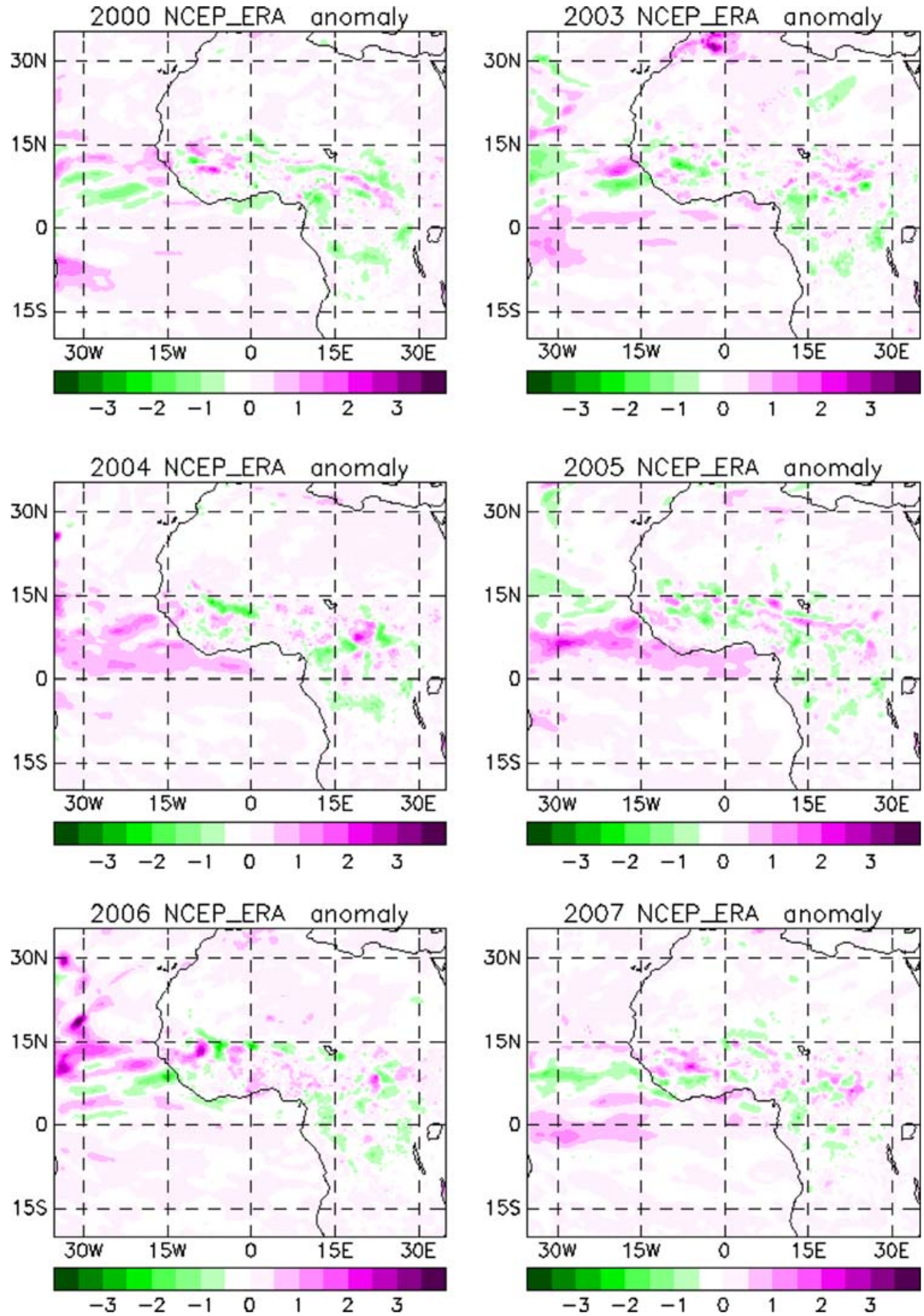

discussed here, is not of sufficient magnitude to have a systematic impact on precipitation. Rather, it appears that these initial SM perturbations generate only random internal variations that have considerable intraseasonal, interannual and spatial variability. Over the Guinea coast region, evapotranspiration is not limited by SM availability, and again the only impact of the initial SM anomalies on precipitation is to generate chaotic variability on a range of time and space scales. In comparison, the impact of the LBCs on the RCM simulations is substantially larger, though perhaps not surprisingly also shows some systematic impact of the slightly different climatology of the driving data.

In summary, we found little sensitivity of WAM precipitation to the specification of initial SM in spring, beyond that due to chaotic internal atmospheric variability. However, this result is likely to be sensitive to the magnitude of the initial perturbation, and could also differ

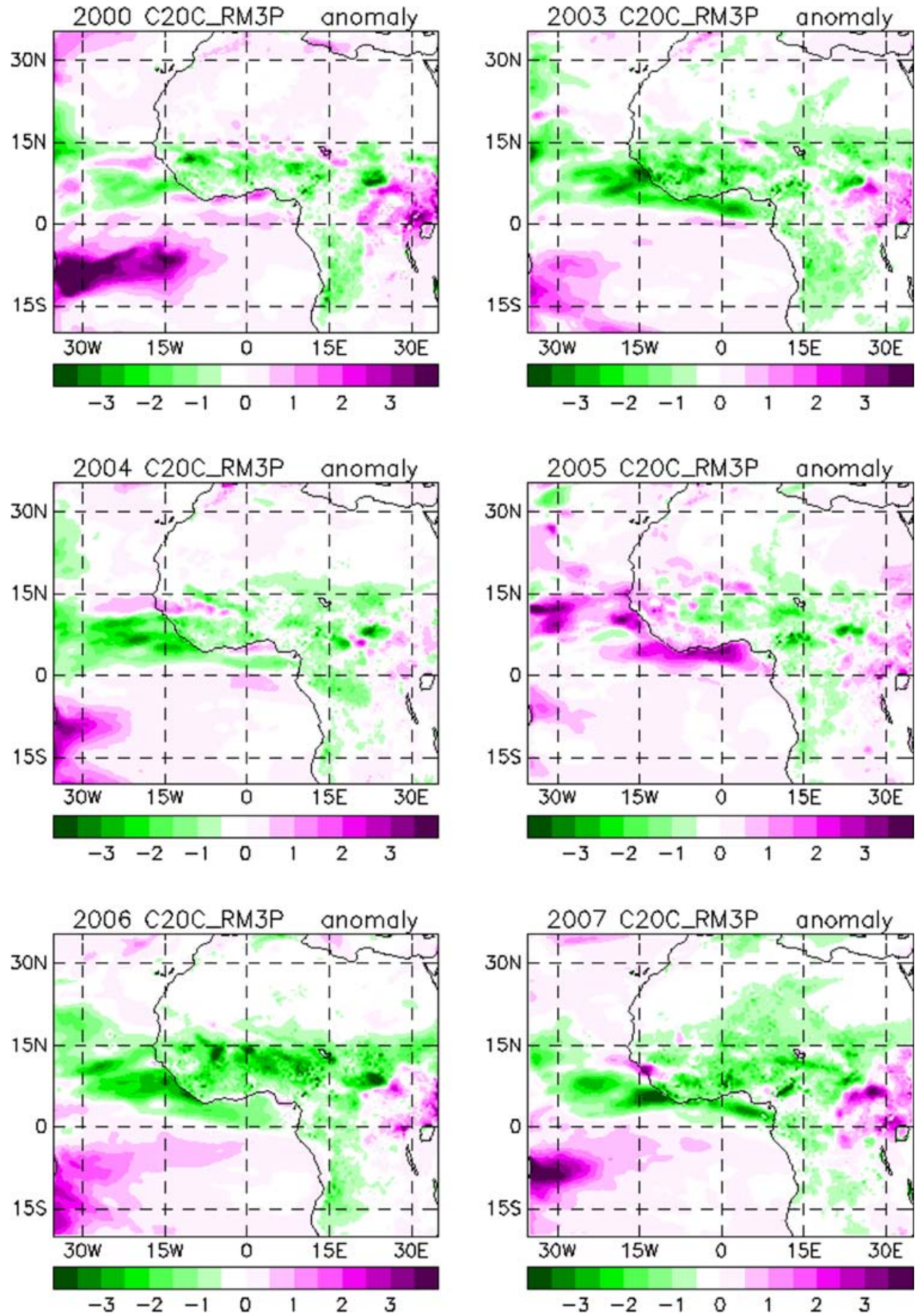

Fig. 11 MJJASO mean precipitation difference, C20C_RM3P minus NCEP_RM3P, (mm/day) for each of the years 2000, 2003–2007

between RCMs. In particular, the initial soil state of the NCEP_ERA experiment derives from a model with the same number of soil layers, and broadly similar depths, to that of HadRM3P. It is possible that the sensitivity to initial SM interpolated from the two-layer NCEP-R2 model may be larger. Therefore, in the context of WAMME discussion on SM initialisation methodologies, we conclude that for HadRM3P it is acceptable to use SM data derived from either an appropriate simulation of the same RCM or interpolated from the ERA-40 reanalysis. But, to verify that this result is applicable to other modelling systems, it would be useful if further studies similarly assess the sensitivity of WAM rainfall to SM initialisation using other models and other sources of SM.

Acknowledgments Discussions with Richard Jones have been much appreciated, along with useful comments from two anonymous reviewers. The work was funded by the Joint DECC, Defra and MoD

Integrated Climate Programme, GA01101, CBC/2B/0417_Annex C5. The NCEP-R2 data used in this study were kindly provided by the NOAA/OAR/ESRL PSD, Boulder, Colorado, USA, from their web site http://www.cdc.noaa.gov/, and the NASA QuikSCAT data were provided by CERSAT-IFREMER, from their web site http://cersat.ifremer.fr/data/.

References

Afiesimama E, Pal J, Abiodun B, Gutowski W, Adedoyin A (2006) Simulation of West African monsoon using the RegCM33. Part I: Model validation and interannual variability. Theor Appl Climatol 86:23–37. doi:10.1007/s00704-005-0202-8

Anderson BT, Kanamaru H, Roads J (2006) Variations in the summertime atmospheric hydrologic cycle associated with seasonal precipitation anomalies over the southwestern US. J Hydrometeor 7:788–807

Anya RO, Semazzi FH, Xie L (2006) Simulated physical mechanisms associated with climate variability over Lake Victoria Basin in East Africa. Mon Wea Rev 134:3588–3609

Biasutti M, Giannini A (2006) Robust Sahel drying in response to late 20th century forcings. Geophys Res Lett 11:L11706. doi:101029/2006GL026067

Christensen OB, Christensen JH, Machenhauer B, Botzet M (1998) Very high resolution regional climate simulations over Scandinavia-present climate. J Clim 11:3204–3227

Cox PM, Betts RA, Bunton CB, Essery RLH, Rowntree PR, Smith J (1999) The impact of new land surface physics on the GCM simulation of climate and climate sensitivity. Clim Dyn 15:183–203

Cuadra SV, da Rocha RP (2007) Sensitivity of regional climatic simulation over Southeaster South America to SST specification during austral summer. Int J Climatol 27:793–804

Dai A, Lamb PJ, Trenberth KE, Hulme M, Jones PD, Xie P (2004) The recent Sahel drought is real. Int J Climatol 24:1323–1331

Denis B, Laprise R, Caya D, Coté J (2002) Downscaling ability of one-way nested regional climate models: the big-brother experiment. Clim Dyn 18:627–646

Dickinson RE, Errico RM, Giorgi F, Bates GT (1989) A regional climate model for the western United States. Clim Change 15:383–422

Douville H (2002) Influence soil moisture on the Asian and African monsoons. Part II: Interannual variability. J Clim 15:701–720

Douville H, Conil S, Tyteca S, Voldoire A (2007) Soil moisture memory and West African monsoon predictability: artifact or reality. Clim Dyn 28(7–8):723–742. doi:10.1007/s00382-006-0208-8

Druyan L, Fulakeza M, Lonergan P (2006) Mesoscale analyses of West African summer climate: focus on wave disturbances. Clim Dyn 27:459–481. doi:10.1007/s00382-006-0141-9

Druyan L, Fulakeza M, Lonergan P (2007) Spatial variability of regional model simulated June–September mean precipitation over West Africa. Geophys Res Lett 34:L18709. doi:10.1029/2007GL031270

Druyan L, Fulakeza M, Lonergan P (2008) The impact of vertical resolution on regional model simulation of the west African summer monsoon. Int J Climatol 28:1293–1314. doi:10.1002/joc.1636

Druyan L, Feng J, Cook KH, Xue Y, Fulakeza M, Hagos SM, Konare A, Moufouma-Okia W, Rowell DP, Vizy EK (2009) The WAMME regional model intercomparison study. Clim Dyn (revised for this issue)

Eltahir EAB, Gong C (1996) Dynamics of wet and dry years in West Africa. J Clim 9:1030–1042

Folland CK, Palmer T, Parker D (1986) Sahel rainfall and worldwide sea temperatures, 1901–85. Nature 320:602–607

Folland CK, Owen J, Ward MN, Coleman A (1991) Prediction of seasonal rainfall in the Sahel region using empirical and dynamical methods. J Forecast 10:21–56

Gallée H, Moufouma-Okia W, Brasseur O, Dupays I, Marbaix P, Messager C, Ramel R, Lebel T (2004) A high resolution simulation of a West African rainy season using a regional climate model. J Geophys Res D05108. doi:10.1029/2003JD004020

Giorgi F (1990) Simulation of regional climate model using a limited area model nested in a general circulation model. J Clim 3:941–963

Giorgi F, Bi X (2000) A study of internal variability of a regional climate model. J Geophys Res 105:29503–29521

Giorgi F, Mearns LO (1999) Introduction to special section: regional climate modeling revisited. J Geophys Res 104:6335–6352

Gochis DJ, Shuttleworth WJ, Yang Z-L (2002) Sensitivity of the modeled North American Monsoon regional climate to convective parameterization. Mon Wea Rev 130:1282–1298

Good P, Lowe JA, Collins M, Moufouma-Okia W (2008) An objective tropical Atlantic sea surface temperature gradient index for studies of south Amazon dry-season climate variability and change. Phil Trans R Soc B 363:1761–1766. doi:10.1098/rstb20070024

Gordon C, Cooper C, Senior CA, Banks H, Gregory JM, Johns TC, Mitchell JFB, Wood RA (2000) The simulation of SST, sea ice extents and ocean heat transports in a version of the Hadley Centre coupled model without flux adjustments. Clim Dyn 16:147–168

Hagos SM, Cook KH (2007) Dynamics of the West African monsoon jump. J Clim 20:5264–5284

Hastenrath (1990) Decadal-scale changes of the circulation in the tropical Atlantic sector associated with Sahel drought. Int J Climatol 10:459–472

Hong SY, Leetma A (1999) An evaluation of the NCEP RSM for regional climate modeling. J Clim 12:592–609

Hong SY, Pan LH (2000) Impact of soil moisture anomalies on seasonal, summertime circulation over North America in a regional climate model. J Geophys Res 105(D24):29625–29634

Huffman GJ, Adler RF, Arkin P, Chang A, Ferraro R, Gruber A, Janowiak J, McNab A, Rudolph B, Schneider U (1997) The global precipitation climatology project (GPCP) combined precipitation data set. Bull Am Meteorol Soc 78:5–20

Janicot S, Moron V, Fontaine B (1996) Sahel droughts and ENSO dynamics. Clim Dyn 18:303–320

Jenkins G (1997) The 1988 and 1990 summer season simulation for West Africa using a regional climate model. J Clim 10:1255–1272

Jones RG, Murphy JM, Noguer M (1995) Simulation of climate change over Europe using a nested regional climate model. I: Assessment of control climate, including sensitivity to location of lateral boundaries. QJR Meteor Soc 121:1413–1449

Jones R, Noguer M, Hassell D, Hudson D, Wilson S, Jenkins G, Mitchell J (2004) Generating high resolution climate change scenarios using PRECIS, Met Office Hadley Centre, Exeter, UK, pp 40

Jung G, Kuntsmann (2007) High-resolution regional climate modeling for the Volta region of West Africa. J Geophys Res 112:D23108. doi:10.1029/2006JD007951

Jung T, Ferranti L, Tompkins AM (2006) Response to the summer of 2003 Mediterranean SST anomalies over Europe and Africa. J Clim 19:5439–5454

Kanamitsu M, Mo KC (2003) Dynamical effect of land surface processes on summer precipitation over the southwestern United States. J. Clim 16:496–509

Kanamitsu M, Ebisuzaki W, Woollen J, Yang SK, Hnilo JJ, Fiorino M, Potter GL (2002) NCEP-DOE AMIP-II reanalysis (R-2), Bull. Am Meteorol Soc 83:1631–1643

Kim JE, Hong SY (2007) Impact of soil moisture anomalies on summer rainfall over East Asia: a regional climate model study. J Clim 20:5732–5743

Koster RD et al (2006) GLACE: the global land–atmosphere coupling experiment. Part I: Overview. J Hydrometeor 6:590–610

L'Hote Y, Mahe G, Some B, Tribouillet JP (2002) Analysis of a Sahelian annual rainfall index updated from 1896 to 2000, the drought still goes on. Hydrol Sci J 47(4):563–572

Laing A, Fritsh JM (1993) Mesoscale convective complexes in Africa. Mon Wea Rev 121:2254–2263

Lamb PJ (1978a) Case studies of tropical Atlantic surface circulation patterns during recent sub-Saharan weather anomalies: 1967 and 1968. Mon Wea Rev 106:482–491

Lamb PJ (1978b) Large-scale tropical Atlantic surface circulation patterns associated with sub-Saharan weather anomalies. Tellus 30:240–251

Lorenz EN (1963) Deterministic nonperiodic flow. J Atmos Sci 20:130–141

McCollum JR, Gruber A, Ba MB (2000) Discrepancy between gauges and satellite estimate of rainfall in Equatorial Africa. J Appl Climatol 39:666–679. doi:10.1175/1520-0450(2000)

Messager C, Gallée H, Brasseur O (2004) Precipitation sensitivity to regional SST in a regional climate simulationduring the West African monsoon for two dry years. Clim Dyn 22:249–266. doi:10.1007/s003820030381

Miguez-Macho G, Stenchikov GL, Robock A (2004) Spectral nudging to eliminate the effect of domain position and geometry in regional model climate simulation. J Geophys Res 109(D13):D13104. doi:10.1029/2003JD004495

Negron Juarez RI, Li W, Fu R, Fernandes K, Cardoso (2009) Comparison of precipitation datasets over Tropical South American and African continents. J Hydrometeor 10:289–299

Nicholson SE, Some B, Kone B (2000) An analysis on recent rainfall conditions in West Africa, including the rainy season of 1997 ENSO year. J Clim 13:2628–2640

Noguer M, Jones R, Murphy J (1998) Sources of systematic errors in the climatology of a regional climate model over Europe. Clim Dyn 14:691–712

Notaro M (2008) Statistical identification of global hot spot in soil moisture feedbacks among IPCC AR4 models. J Geophys Res 113: D09101. doi:10.1029/2007JD009199

Nunes AM, Roads JO (2007) Influence of precipitation assimilation on a regional climate model surface water and energy budgets. J Hydrometeor 8(5):642–664

Paegle J, Mo KC, Nogués-Paegle (1996) Dependence of simulated precipitation on surface evaporartion during the 1993 United States summer floods. Mon Wea Rev 124:345–361

Paeth H, Hense A (2004) SST versus climate change signals in West African rainfall: 20th century variations and future projections. Clim Change 66:179–208

Paeth H, Born K, Podzun R, Jacob (2005) Regional downscaling over West Africa: Model evaluation and comparison of wet and dry years. Meteorol Z 14:349–367

Palmer TN (1986) Influence of Atlantic, Pacific and Indian Oceans on Sahel rainfall. Nature 322:251–253

Pan HL (1990) A simple parameterization scheme of evapotranspiration over land for the NMC medium-range forecast model. Mon Wea Rev 118:2500–2512

Pope VD, Gallani ML, Rowntree PR, Stratton RA (2000) The impact of new physical parametrizations in the Hadley Centre climate model: HadAM3. Clim Dyn 16:123–146. doi:10.1007/s003820050009

Ramel R, Gallée H, Messager C (2006) On the northward shift of the West African monsoon. Clim Dyn 26:429–440. doi:10.1007/s00382-005-0093-5

Rayner NA, Parker DE, Horton EB, Folland CK, Alexander LV, Rowell DP, Kent EC, Kaplan A (2003) Global analyses of SST, sea ice and night marine air temperature since the late nineteenth century. J Geophys Res 108:(D14) 4407. doi:10.1029/2002JD002670

Redelsperger JL, Thorncroft CD, Diedhiou A, Lebel T, Parker DJ, Polcher J (2006) African Monsoon Multidisciplinary Analysis–An international research project and field compaign. Bull Am Meteorol Soc 87:1739–1746

Rojas M, Seth A (2003) Simulation and sensitivity in a nested modeling system for tropical South America. Part II: GCM boundary forcing. J Clim 16:2454–2471

Rowell DP (2001) Teleconnections between the tropical Pacific and the Sahel. QJR Meteor Soc 127:1683–1706

Rowell DP (2003) The impact of Mediterranean SSTs on the Sahelian rainfall season. J Clim 16:849–862

Rowell DP, Jones RG (2006) Causes and uncertainty of future summer drying over Europe. Clim Dyn 27:281–299

Rowell DP, Folland CK, Maskell K, Ward MN (1995) Variability of summer rainfall over tropical North Africa (1906–92): observations and modelling. QJR Meteor Soc 121:669–704

Semazzi FH, Mehta V, Sud YC (1988) An investigation of the relationship between Sub-Saharan rainfall and global sea surface temperature. Atmos-Ocean 26:118–138

Seneviratne SI, Pal JS, Eltahir EAB, Schär C (2002) Summer dryness in a warmer climate: a process study with a regional climate model. Clim Dyn 20:69–85

Seth A, Giorgi F (1998) The effect of domain choice on summer precipitation simulation and sensitivity in a regional climate model. J Clim 11:2698–2712

Seth A, Rojas M (2003) Simulation and sensitivity in a nested modeling system for tropical South America. Part I: reanalyses boundary forcing. J Clim 16:2437–2453

Shinoda M, Kawamura R (1994) Tropical rainbelt, circulation, and sea surface temperatures associated with the Sahelian rainfall trend. J Meteorol Soc Jpn 72:341–357

Sijikumar S, Roucou P, Fontaine B (2006) Monsoon onset over Sudan–Sahel: simulation by the regional scale model MM5. Geophys Res Lett 33:L03814. doi:10.1029/2005GL024819

Simmons AJ, Gibson JK (2000) The ERA-40 project plan. ERA-40 Project Report Series 1. Shinfield Park, UK, p 63

Taylor KE, Williamson D, Zwiers F (2000) The sea surface temperature and sea-ice concentration boundary conditions for AMIP II simulations. PCMDI Report No. 60. Lawrence Livermore National Laboratory, Livermore 25 pp

Trenberth KE, Large WG, Olson JG (1990) The mean annual cycle in global ocean wind stress. J Phys Oceanogr 20:1742–1760

Van den Hurk BJJM, Viterbo P, Beljaars ACM, Betts AK (2000) Offline validation of the ERA-40 surface scheme. ECMWF Tech Memo 295, 42 pp

Vannitsem S, Chomé F (2005) One-way nested regional climate simulations and domain size. J Clim 18:229–233

Vanvyve E, Hall N, Messager C, Leroux S, Ypersele J-P (2007) Internal variability in a regional climate model over West africa. Clim Dyn. doi:10.1007/s00382-007-0281-6

Vizy EK, Cook KH (2001) Mechanism by which Gulf of Guinea and eastern North Atlantic sea surface temperature anomalies can influence African rainfall. J Clim 15:795–821

Vizy EK, Cook KH (2002) Development and application of a mesoscale climate model for the tropics: influence of sea surface temperature anomalies on the West African monsoon. J Geophys Res 107(D3): 4023. doi:10.1029/2001JD000686

Wang Y, Xu H, Xie S-P (2004) Regional model simulations of marine boundary layer clouds over the Southeast Pacific off South America. Mon Wea Rev 132:2650–2668

Ward MN (1994) Tropical North Atlantic rainfall and worldwide monthly to multi-decadal climate variations. PhD thesis, University of Reading, p 313

Xu J, Shuttleworth WJ, Gao X, Sorooshian S, Small EE (2004) Soil moisture-precipitation feedback on the North American monsoon system in MM5-OSU model. QJR Meteorol Soc 130:2873–2890

Xue Y, Juang HM, Li WP, Prince S, DeFries R, Jiao Y, Vasic R (2004) Role of land surface processes in monsoon development: East Asia and West Africa. J Geophys Res 109. doi:10.1029/2003JD003556

Xue Y, Lau K-M, Cook K, Rowell DP, Boone A, Feng J, Konare A, Bruecher T, De Sales F, Dirmeyer P, Druyan L, Fink A, Fulakeza M, Guo Z, Hagos S, Kim K-M, Kitoh A, Kumar V, Lonergan P, Pasqui M, Poccard-Leclercq I, Mahowald N, Moufouma-Okia W, Pegion P, Sanda I, Schemm J, Schubert S, Sealy A, Thiaw W, Vintzileos A, Vizy E, Williams S, Wu M-L (2009) The West African Monsoon Modeling and Evaluation project (WAMME) and its First Model Intercomparison Experiment. Bull Am Meteorol Soc (Submitted)

Yhang Y-B, Hong S-Y (2008) Improved physical processes in a regional climate model and their impact on the simulated summer monsoon circulation over East Asia. J Clim 21:963–979